The Scientific Temper (2024) Vol. 15 (3): 2416-2420
E-ISSN: 2231-6396, ISSN: 0976-8653
Doi: 10.58414/SCIENTIFICTEMPER.2024.15.3.01
https://scientifictemper.com/

RESEARCH ARTICLE

Positive impact of using α-Fe_2O_3 nanoparticles as dietary supplements on some hematological parameters of an economically important minor carp *Labeo bata* (Hamilton, 1822)

Sampa Mondal[1*], Nilanjana Chatterjee[2], Baibaswata Bhattacharjee[3]

Abstract

A simple, low-cost wet chemical method is employed to synthesize α-Fe_2O_3 nanoparticles (NPs) and different samples are synthesized by varying the calcination temperature. Microstructural characterizations confirm the excellent quality of synthesized α-Fe_2O_3 NPs having different sizes. The synthesized NPs are used as dietary supplements of an economically important minor carp *Labeo bata* (F. Hamilton, 1822), to investigate the effects on some hematological parameters (hemoglobin, red blood corpuscle, and hematocrit) of the fish. Significant improvements in hemoglobin (Hb), red blood corpuscle (RBC), and hematocrit (Hct), are observed owing to the treatment with α-Fe_2O_3 NPs. Increasing Hb, RBC, and Hct can be associated with the increased absorption of iron in its nano form into the fish body *via* dietary supplements. Our data further demonstrate that the hematological effect of *L. bata* becomes more favorable as the concentration of NPs rises and or the size of the NPs falls, up to a certain level.

Keywords: Iron oxide nanoparticles, *Labeo bata*, Hemoglobin, Red blood corpuscle, Hematocrit.

Introduction

Iron is a vital ingredient for fish growth and the development of improved physiological and immunological properties (Shenawy *et al*., 2019; Farahmandjou & Soflaee, 2015). This micronutrient is essential for oxygen transport and cellular respiration via oxidation-reduction and electron transfer (Roos *et al*., 2007). Iron deficiency can cause physiological difficulties in animals (Y.L. Guo *et al*., 2017, 2018). Supplemented feed increases the nutritional composition and aquatic species' ability to consume, digest, and absorb nutrients (Roos *et al*., 2007; Shenawy *et al*., 2019). Fish require iron supplements because their dietary requirements do not match the levels available in natural iron sources due to low solubility and bioavailability (Y.L. Guo *et al*., 2018). Hematite (α-Fe2O3) is the most stable iron oxide and a beneficial environmental semiconductor (Sangaiya & Jayaprakash, 2018). Worldwide production of α-Fe_2O_3 NPs is expanding exponentially because of their unique physicochemical characteristics (L. Guo *et al*., 2018).

In the present study, α-Fe_2O_3 NPs are synthesized utilizing a simple, low-cost wet chemical process, and different samples are synthesized with varying annealing temperatures. Throughout the year, *Labeo bata* is given supplemental α-Fe_2O_3 NPs at 0 (control), 0.5, 1, 1.5, and 2 g/kg diet. Because of their nanostructure, the micronutrients in α-Fe_2O_3 NPs are easily absorbed by fish cells from their diet, producing high-protein fish that greatly benefit both the environment and human civilization. The positive effects under treatment with α-Fe_2O_3 NPs on some hematological parameters of economically important minor carp *L. bata* (F. Hamilton, 1822) are observed. In this research, *L. bata* is used due to its economic and ecological significance (Debnath *et al*., 2022; Karnatak *et al*., 2021). To the best of our knowledge,

[1]Department of Physics, Bankura Zilla Saradamani Mahila Mahavidyapith, Bankura, West Bengal, India

[2]Department of Zoology, Ramananda College, Bishnupur, Bankura, West Bengal, India

[3]Department of Physics, Ramananda College, Bishnupur, Bankura, West Bengal, India

***Corresponding Author:** Sampa Mondal, Department of Physics, Bankura Zilla Saradamani Mahila Mahavidyapith, Bankura, West Bengal, India, E-Mail: sampa.mondal998@gmail.com

How to cite this article: Mondal, S., Chatterjee, N., Bhattacharjee, B. (2024). Positive impact of using α-Fe_2O_3 nanoparticles as dietary supplements on some hematological parameters of an economically important minor carp *Labeo bata* (Hamilton, 1822). The Scientific Temper, **15**(3):2416-2420.

Doi: 10.58414/SCIENTIFICTEMPER.2024.15.3.01

Source of support: Nil

Conflict of interest: None.

Received: 25/07/2024 **Accepted:** 28/08/2024 **Published**: 10/09/2024

this is the first report on the hematological study of *L. bata* under treatment with α-Fe_2O_3 NPs. However, iron oxide NPs have highly beneficial effects on hematological parameters, and these benefits vary with experimental design up to a specific level. Under the same conditions, increasing the concentration of α- Fe_2O_3 NPs leads to increased Hb, RBC, and Hct up to a certain level. Furthermore, as the size of the NPs increases, the positive effect on hematological parameters reduces gradually.

Materials and Methods

Synthesis and Characterizations of α-Fe_2O_3 NPs

Firstly, 0.04 M of ferric chloride hexahydrate ($FeCl_3 \cdot 6H_2O$) (Merck, purity 99.99%) is dissolved in 250 mL of DI water (Merck, purity 99.99%) under continual stirring at room temperature. After that, 6.5 mL of sodium hydroxide (NH_4OH) solution (Merck, purity 99.99%) is mixed dropwise into the $FeCl_3 \cdot 6H_2O$ solution. The resulting reddish-black solution is stirred for an additional 4 hours. This solution is then filtered with Whatman No. 1 filter paper to obtain the precipitates, which are washed four times with DI water. The precipitates are then heated at 90℃ until they become completely dry. After that, the dried samples are annealed in a muffle furnace for 3 hours at a specific temperature according to the experimental design Table 1. To obtain the samples in the form of fine powder, finally, the samples are grounded.

A BTI-35 muffle furnace (GMP model) is used to anneal the dried sample. Using a Bruker D8 Advance diffractometer, the crystallinity of the α-Fe_2O_3 NPs is assessed throughout an angular range (2θ) of 20-70°. A Zeiss Sigma field-enhanced secondary electron microscope (FESEM) is used to examine the morphology of the produced NPs. A Jasco V-770 spectrophotometer is used to record UV-vis absorption spectra spanning the wavelength range of 500 to 1000 nm.

Fish Husbandry

L. bata fish hatchling specimens are acquired from local fishermen and promptly transferred to completely waterproof containers filled with disinfected tap water and left to stand for a few days. The setup is supplied with the appropriate oxygen supply. To produce a natural habitat, the water's temperature is kept between 25 to 30℃. A small amount of genuine fish food (Table 2) is fed to the fish regularly. The fish are acclimatized to the laboratory environment for ten days before the tests begin. Measurement of Hb, RBC, and Hct are done for treated fish as well as control fish in late May.

Table 1: Design of experiment for the formation of α-Fe_2O_3 NPs and sample name of different α-Fe_2O_3 NPs according to the experimental conditions

Annealing temperature (℃)	*Sample name*
400	Sample – 1
450	Sample – 2
500	Sample – 3
550	Sample– 4

Table 2: Preparation of fish feed: Composition of our experimental diet for the fish feed

Ingredients	*Dry weight percentage*
Casein (protein source)	30.0
Gelatin (protein source)	8.0
Fat [soyabean oil and menhaden fish oil (1:1) with 0.001% Ethoxyquin]	4.5
Cellulose	8.0
Dextrin	37.5
Carboxy methyl cellulose	5.0
Choline chloride	0.5
Mineral premix	4.5
Vitamin premix	2.0

Table 3: Included diet with each α-Fe_2O_3 NPs supplement for different experimental groups

Experimental groups	*Included diet with iron oxide supplement according to concentration*
Control group	0 g/kg dry feed weight
Treatment 1	0.5 g/kg dry feed weight
Treatment 2	1 g/kg dry feed weight
Treatment 3	1.5 g/kg dry feed weight
Treatment 4	2 g/kg dry feed weight

Experimental Exposure

Fish are separated into five groups, each with a population of 10 fish, after 10 days of collecting. Then, *L. bata* is fed supplementary α-Fe_2O_3 NPs of different particle sizes at rates of zero (control), 0.5, 1, 1.5, and 2 g/kg diet throughout the year (Table 3). This full treatment is designed for different α-Fe_2O_3 NPs having particle sizes 8, 10, 13, and 16 nm to observe the effect of particle size on hematological parameters. The study compares the hematological effect on the fish at four different concentrations of α-Fe_2O_3 NPs to the control group. The impact of α-Fe_2O_3 NPs on the hematological parameters of *L. bata* is characterized by comparing the Hb, RBC, and Hct of the fish under treatment with α-Fe_2O_3 NPs of different concentrations to that of the fish living in controlled conditions.

Preparation of Blood Samples

To prepare the blood film, a drop of blood is placed on the edge of a clean, grease-free slide, and then a spreader is used to evenly distribute the blood film over the slide in a horizontal direction. After allowing the blood film to air dry, Leishman's stain is applied to it to count and depict the red

blood cells. In this way, slides of blood samples of fish under control and treatment are prepared. Stress was minimized as much as possible when sampling.

Fish from the control and iron oxide-treated aquariums are taken out and blood is collected by the heart puncture using a plastic disposable syringe. Blood samples are taken from 10 separate fish samples from the control and iron oxide-treated aquariums by puncturing the caudal vein using a 20 G×1.5 disposable syringe. These samples are collected in a microtube with ethylenediaminetetraacetic acid (EDTA) (ratio 1.26 mg/0.6 mL) as the anticoagulant.

The blood samples from microtubes are utilized to estimate hematological parameters such as Hb, RBC, and Hct counts.

Hematological Parameters

All hematological profiles are computed within one hour of the blood sample being collected using an automated hematology analyzer (HeCo Vet C, SEAC, Florence, Italy) with a proper lysing reagent for fish (SEAC, Code 71010460), previously used to investigate hematological profile in other fish (Fazio *et al*., 2016). The hemogram is used to determine parameters such as Hb concentration, RBC, and Hct.

Statistical Analysis

A one-way analysis of variance is performed to examine the variations between experimentally treated groups and control groups. When $p < 0.001$, differences are deemed statistically significant. At a level of significance of 5%, Pearson's correlation coefficients (r) are computed to see if there is any link at all between the various experimental parameters and the concentrations, sizes, and feeding durations of NPs. In the manuscript, positive values are used without any prefix, while negative r values are prefixed with a negative (-) symbol. Origin 9 is used to fit a curve to the experimentally collected data.

Results and Discussion

X-ray diffraction

The X-ray diffraction (XRD) spectrum of all the samples along with the standard, are shown in Figure 1. The presented peaks for all the samples match well with the (012), (104), (110), (113), (024), (116), (214), and (300) planes of a hexagonal structure of α- Fe_2O_3 NPs, identified using standard data (JCPDS 33-0664) (Rao *et al*., 2013). Any of the XRD spectra doesn't show any additional peak confirming the existence of pure phase in all the Fe_2O_3 NPs. The mean size of the NPs is determined using the Debye-Sherrer formula and the following equation (Bhattacharyya *et al*., 2011; Kumar *et al*., 2023; Ounacer *et al*., 2020; Rachmaniar *et al*., 2024; V. Samuthira Pandi *et al*., 2023):

$$D = \frac{0.89\,\lambda}{\beta\,\cos\theta} \quad (1)$$

where θ is the Bragg angle, λ is the wavelength of the Cu K_α X-radiation, β is the full width at half maximum (FWHM) of the diffraction peaks and the shape factor is 0.89. The calculated mean particle sizes of different samples are given in Table 4.

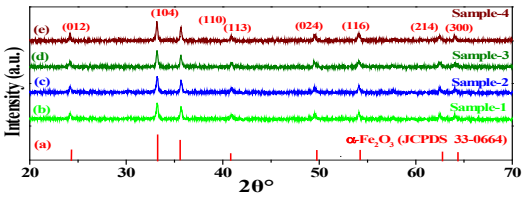

Figure 1: XRD pattern of (a) standard hematite, (b) sample-1, (c) sample-2, (d) sample-3, (e) sample-4

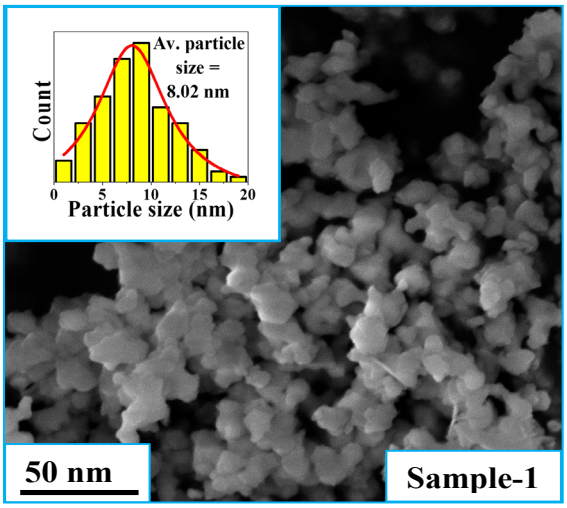

Figure 2: FESEM images of sample-1; 2 (inset): particle size distribution histograms of corresponding NPs

Table 4: Estimated particle size from XRD and SEM and energy band gap of α-Fe_2O_3 NPs obtained under different experimental conditions

Sample name	*Average particle size (nm) from XRD*	*Average particle size (nm) from SEM*	*Band gap energy (eV)*
Sample – 1	8	8.02	2.90
Sample – 2	10	9.89	2.82
Sample – 3	13	13.24	2.78
Sample– 4	16	15.87	2.73

Morphological Investigation

Figure 2 shows the FESEM image with the corresponding particle size distribution data of sample-1. Well-dispersed NPs are visible in the micrograph. The shapes of the majority of α-Fe_2O_3 NPs are found to be spherical or oval. The morphological study is done utilizing the FESEM image and the particle size distribution histogram is obtained. The estimated average particle sizes of the synthesized sample obtained from the particle size distribution data are given in Table 4.

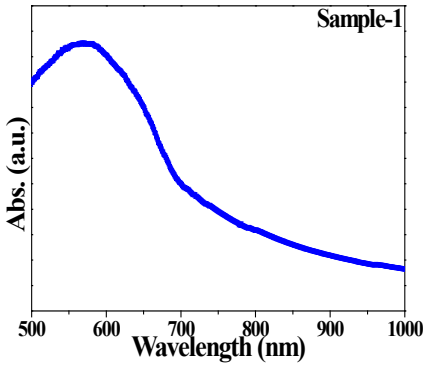

Figure 3: UV-vis spectra of sample-1

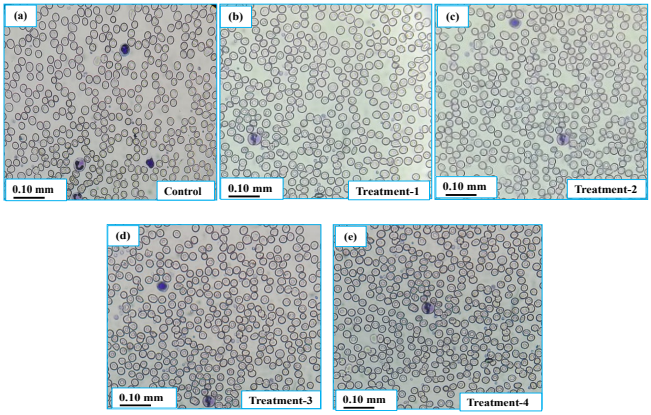

Figure 4: Microscopic view of blood film of *L. bata* under different experimental conditions: (a) control group, (b) treatment-1, (c) treatment-2, (d) treatment-3, (e) treatment-4 for nanoparticle size 8 nm

UV-vis spectroscopy

The board absorption spectra throughout the UV region of the produced α-Fe_2O_3 NPs for different synthesis methods are shown in Figure 3. The energy-dependent absorption coefficient (α) is the foundation of the Tauc method. The optical bandgaps of the as-prepared α-Fe_2O_3 NPs are estimated using the Tauc plot by plotting $(\alpha h\nu)^2$ against hν and extrapolating the band edge slope against zero (Awais *et al*., 2023; Hammad *et al*., 2022; Parimala & Ganeshkumar, 2024; Yasmin *et al*., 2021). The estimated optical bandgaps of samples are given in Table 4.

Hematological Findings

The microscopic images of blood films are shown in Figure 4. Figures 4a, 4b, 4c, 4d and 4e can be used to calculate the concentration of RBC of *L. bata* under control, treatment-1, treatment-2, treatment-3 and treatment-4 conditions, respectively (for particle size 8 nm). After the treatment, it turns out that the concentration of RBC increases compared with fish living in natural conditions (Figure 4). Additionally, the concentration of RBC increases with rising α-Fe_2O_3 NPs concentration.

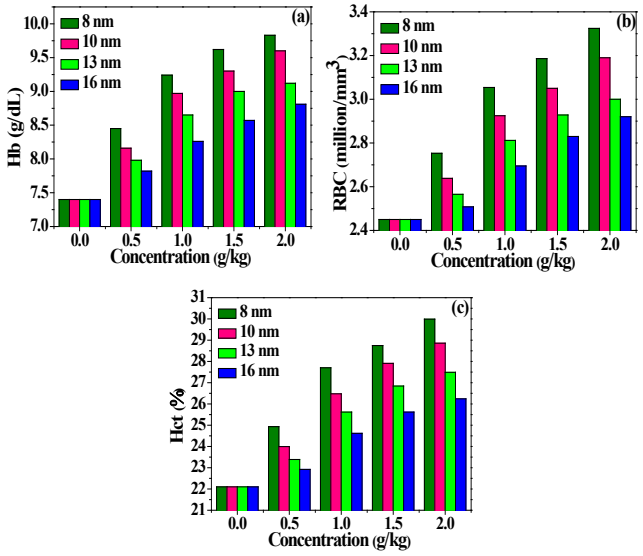

Figure 5: Variation of hematological parameters of *L. bata* under different experimental conditions with increasing concentration α-Fe_2O_3 NPs: (a) Hb, (b) RBC, and (c) Hct

Figures 5a, 5b, and 5c show that Hb, RBC, and Hct of *L. bata* significantly change ($p < 0.001$) as the concentration of NPs rises for different experimental groups. However, Hb, RBC, and Hct are enhanced as the concentration increases up to 2 g/kg diet and or the NPs size falls to 8 nm. The treatments show that the highest value of Hb, RBC, and Hct of fish at about 9.84 g/dL (Figure 5a), 3.32 million/mm^3 (Figure 5b), and 29.99% (Figure 5c), respectively, are observed for sample-1 (particle size 8 nm) at 2 g/kg diet concentration. This positive result indicates that the α-Fe_2O_3 NPs supplementations are offering favorable conditions. Above the concentration of 2 g/kg diet, the positive impact on hematological parameters becomes stable for each NPs. And with increasing particle size the favourable impact becomes less notable.

Conclusion

α-Fe_2O_3 NPs are synthesized using a simple wet chemical method and different samples are synthesized with changing annealing temperature. SEM and XRD investigations confirm the outstanding quality of α-Fe_2O_3 NPs. With varied NPs concentrations, the hematological effect of *L. bata* shows remarkable changes under identical circumstances. The Hb, RBC, and Hct of fish increase with increasing the concentration of NPs up to 2 g/kg diet. The treatments show that the maximum values of Hb, RBC, and Hct of *L. bata* at about 9.84 g/dL, 3.32 million/mm^3, and 29.99%, respectively, are observed for 8 nm particle size at 2 g/kg diet concentration. The hematological parameters of *L. bata* are almost stable beyond this concentration. This positive impact becomes less noticeable with increasing particle size from 8 nm. Additionally, this impact gradually diminishes with increasing NPs sizes. To sum up, the current research

findings unequivocally show that α-Fe_2O_3 NPs added to a baseline diet have the potential to serve as a substitute source for correcting an iron shortage in *L. bata*.

Acknowledgment

The authors would like to acknowledge the Co-ordinator, Centre of Excellence in Advanced Materials, National Institute of Technology, Durgapur, for microstructural characterization.

References

Awais, S., Munir, H., Najeeb, J., Anjum, F., Naseem, K., Kausar, N., Shahid, M., Irfan, M., & Najeeb, N. (2023). Green synthesis of iron oxide nanoparticles using Bombax malabaricum for antioxidant, antimicrobial and photocatalytic applications. *Journal of Cleaner Production*, *406*, 136916. https://doi.org/10.1016/j.jclepro.2023.136916

Bhattacharyya, A., Datta, P. S., Bhaumik, A., Viraktamath, S., Chowdhury, M. U., & Isaac, R. K. (2011). TINY DEVICES-NANO - THE EMERGING WORLD TECHNOLOGY. *The Scientific Temper*, *2*(1 & 2), 9–14. https://doi.org/10.58414/SCIENTIFICTEMPER.2011.02.1.02

Debnath, D., Das, B. K., Yengkokpam, S., Das, P., Yadav, A. K., Sharma, N., Borah, S., Ray, B. C., Kakati, A., Sarkar, U. K., & Bhattacharjya, B. K. (2022). Evaluating growth, production and economics of a new candidate species *Labeo bata* in cages: A regional model for table fish production in floodplain wetlands of North East India. *Aquaculture*, *546*, 737344. https://doi.org/10.1016/j.aquaculture.2021.737344

Farahmandjou, M., & Soflaee, F. (2015). Synthesis and characterization of α-Fe2O3 Nanoparticles by Simple Co-Precipitation Method. *Physical Chemistry Research*, *3*(3). https://doi.org/10.22036/pcr.2015.9193

Fazio, F., Saoca, C., Piccione, G., Kesbic, O. S., & Acar, U. (2016). Comparative Study of Some Hematological and Biochemical Parameters of Italian and Turkish Farmed Rainbow Trout Oncorhynchus mykiss (Walbaum, 1792). *Turkish Journal of Fisheries and Aquatic Sciences*, *16*(3). https://doi.org/10.4194/1303-2712-v16_3_25

Guo, L., Chen, H., He, N., & Deng, Y. (2018). Effects of surface modifications on the physicochemical properties of iron oxide nanoparticles and their performance as anticancer drug carriers. *Chinese Chemical Letters*, *29*(12), 1829–1833. https://doi.org/10.1016/j.cclet.2018.10.038

Guo, Y.L., Jiang, W.-D., Wu, P., Liu, Y., Zhou, X.-Q., Kuang, S.-Y., Tang, L., Tang, W.-N., Zhang, Y.-A., & Feng, L. (2017). The decreased growth performance and impaired immune function and structural integrity by dietary iron deficiency or excess are associated with TOR, NF-κB, p38MAPK, Nrf2 and MLCK signaling in head kidney, spleen and skin of grass carp (Ctenopharyngodon idella). *Fish & Shellfish Immunology*, *65*, 145–168. https://doi.org/10.1016/j.fsi.2017.04.009

Guo, Y.L., Wu, P., Jiang, W.-D., Liu, Y., Kuang, S.-Y., Jiang, J., Tang, L., Tang, W.-N., Zhang, Y.-A., Zhou, X.-Q., & Feng, L. (2018). The impaired immune function and structural integrity by dietary iron deficiency or excess in gill of fish after infection with Flavobacterium columnare: Regulation of NF-κB, TOR, JNK, p38MAPK, Nrf2 and MLCK signalling. *Fish & Shellfish Immunology*, *74*, 593–608. https://doi.org/10.1016/j.fsi.2018.01.027

Hammad, E. N., Salem, S. S., Mohamed, A. A., & El-Dougdoug, W. (2022). Environmental Impacts of Ecofriendly Iron Oxide Nanoparticles on Dyes Removal and Antibacterial Activity. *Applied Biochemistry and Biotechnology*, *194*(12), 6053–6067. https://doi.org/10.1007/s12010-022-04105-1

Karnatak, G., Das, B. K., Mishal, P., Tayung, T., Kumari, S., Sarkar, U. K., Das, A. K., & Ali, Y. (2021). Impact of stocking density on growth, feed utilization and survival of cage reared minor carp, *Labeo bata* (Hamilton, 1822) in Maithon reservoir, India. *Aquaculture*, *532*, 736078. https://doi.org/10.1016/j.aquaculture.2020.736078

Kumar, N., Vikram Delu, Tarsem Nain, Anil Kumar, Pooja, & Arbind Acharya. (2023). Exploring the therapeutic implications of nanoparticles for liquid tumors: A comprehensive review with special emphasis on green synthesis techniques in the context of Dalton's lymphoma. *The Scientific Temper*, *14*(03), 916–926. https://doi.org/10.58414/SCIENTIFICTEMPER.2023.14.3.55

Ounacer, M., Essoumhi, A., Sajieddine, M., Razouk, A., Costa, B. F. O., Dubiel, S. M., & Sahlaoui, M. (2020). Structural and Magnetic Studies of Annealed Iron Oxide Nanoparticles. *Journal of Superconductivity and Novel Magnetism*, *33*(10), 3249–3261. https://doi.org/10.1007/s10948-020-05586-z

Parimala, V., & Ganeshkumar, D. (2024). Solar energy-driven water distillation with nanoparticle integration for enhanced efficiency, sustainability, and potable water production in arid regions. *The Scientific Temper*, *15*(01), 1644–1651. https://doi.org/10.58414/SCIENTIFICTEMPER.2024.15.1.11

Rachmaniar, S., Nugraha, D. A., Santjojo, D. J. D. H., Tjahjanto, R. T., Mufti, N., & Masruroh. (2024). Prevention of particle agglomeration in sol–gel synthesis of TiO2 nanoparticles via addition of surfactant. *Journal of Nanoparticle Research*, *26*(3), 45. https://doi.org/10.1007/s11051-024-05943-2

Rao, X., Su, X., Yang, C., Wang, J., Zhen, X., & Ling, D. (2013). From spindle-like β-FeOOH nanoparticles to α-Fe2O3 polyhedral crystals: Shape evolution, growth mechanism and gas sensing property. *CrystEngComm*, *15*(36), 7250. https://doi.org/10.1039/c3ce40430g

Roos, N., Thorseng, H., Chamnan, C., Larsen, T., Gondolf, U. H., Bukhave, K., & Thilsted, S. H. (2007). Iron content in common Cambodian fish species: Perspectives for dietary iron intake in poor, rural households. *Food Chemistry*, *104*(3), 1226–1235. https://doi.org/10.1016/j.foodchem.2007.01.038

Sangaiya, P., & Jayaprakash, R. (2018). A Review on Iron Oxide Nanoparticles and Their Biomedical Applications. *Journal of Superconductivity and Novel Magnetism*, *31*(11), 3397–3413. https://doi.org/10.1007/s10948-018-4841-2

Shenawy, A., Gad, D., & Yassin, S. (2019). Effect of Iron Nanoparticles on the Development of Fish Farm Feeds. *Alexandria Journal of Veterinary Sciences*, *60*(1), 102. https://doi.org/10.5455/ajvs.28123

V.Samuthira Pandi, B. R. Senthil Kumar, Anusuya, M., & Annu Dagar. (2023). Synthesis and characterization of ZnO, ZnO doped Ag2O nanoparticles and its photocatalytic activity. *The Scientific Temper*, *14*(03), 827–833. https://doi.org/10.58414/SCIENTIFICTEMPER.2023.14.3.41

Yasmin, S. R., Verma, Y., & Lawrence, R. (2021). Biowaste-derived Nanoparticles and Their Preparation: A Review. *The Scientific Temper*, *12*(1 & 2). https://doi.org/10.58414/SCIENTIFICTEMPER.2021.12.1.02